

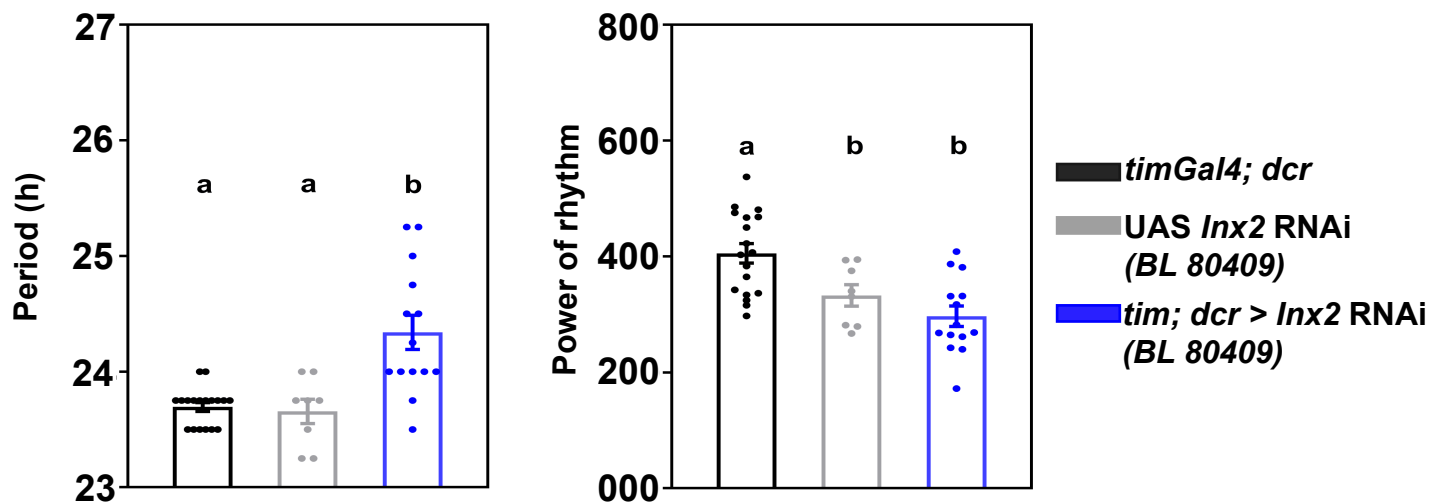
iScience, Volume 24

Supplemental information

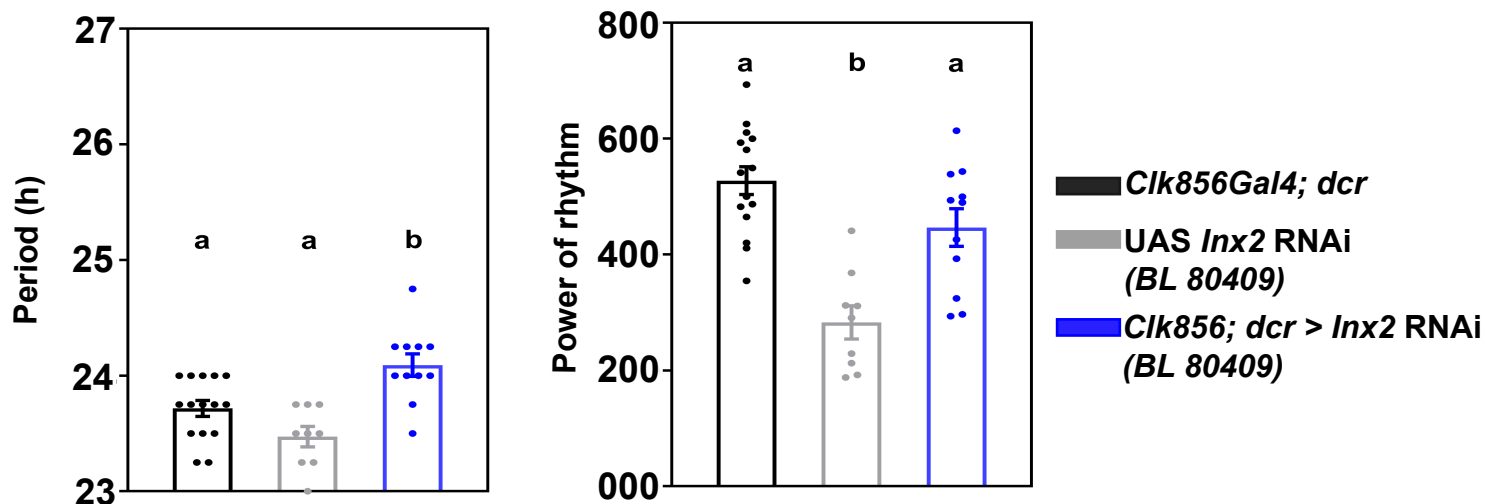
**Gap junction protein Innexin2 modulates
the period of free-running rhythms
in *Drosophila melanogaster***

Aishwarya Ramakrishnan and Vasu Sheeba

A

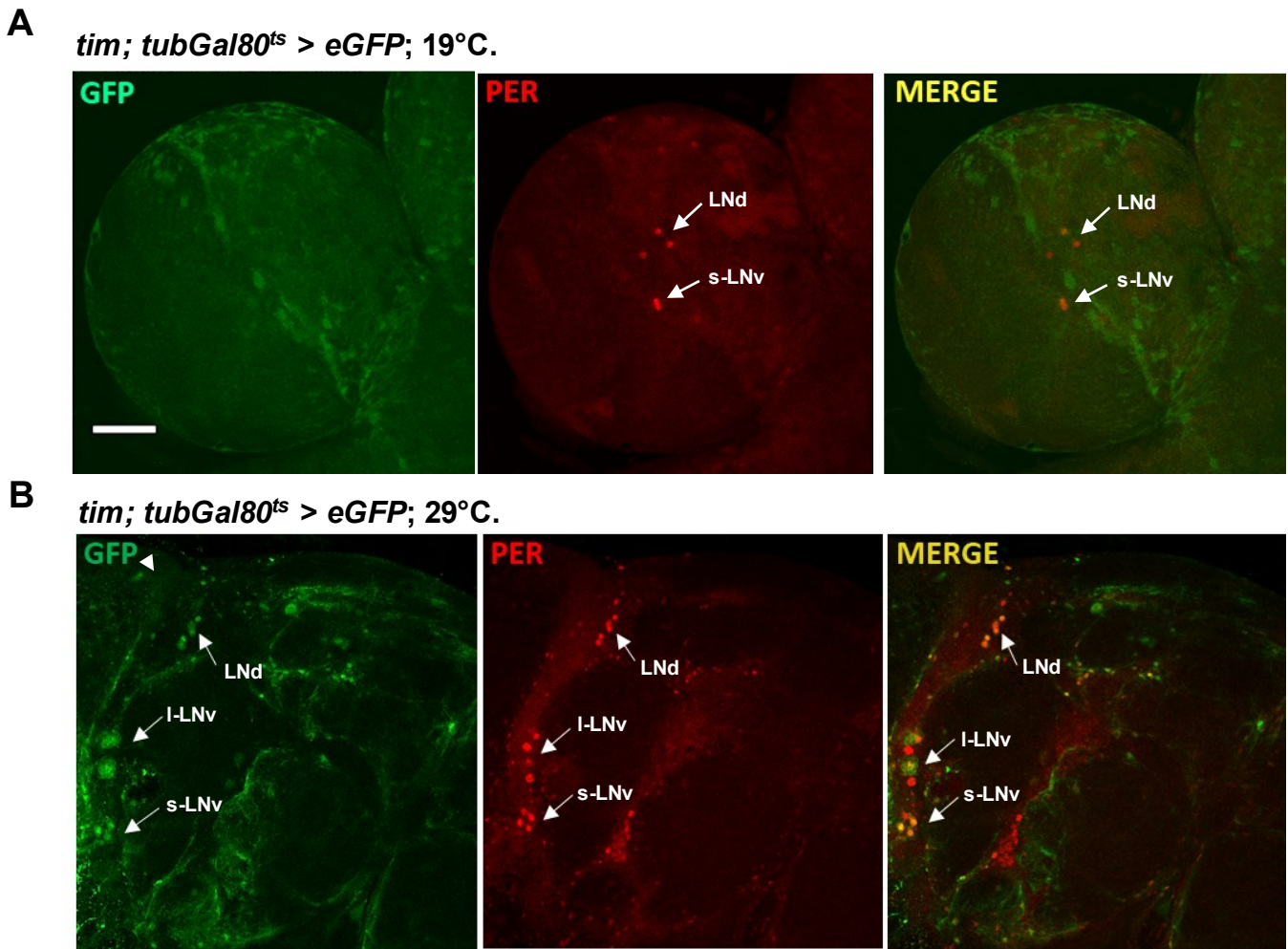


B

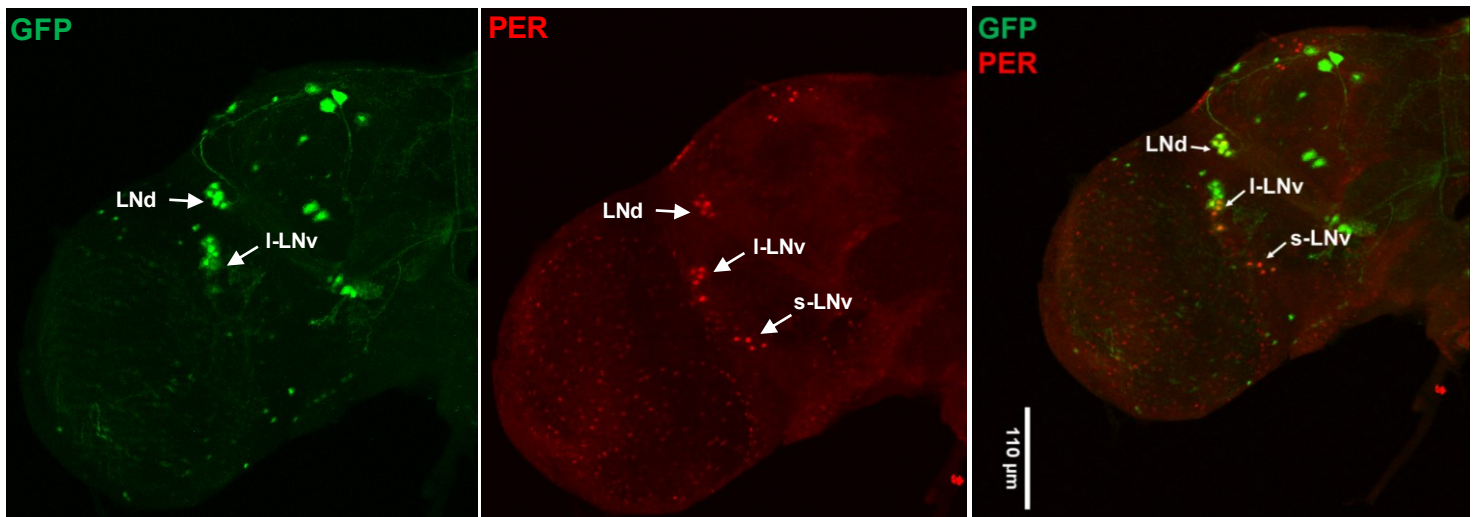
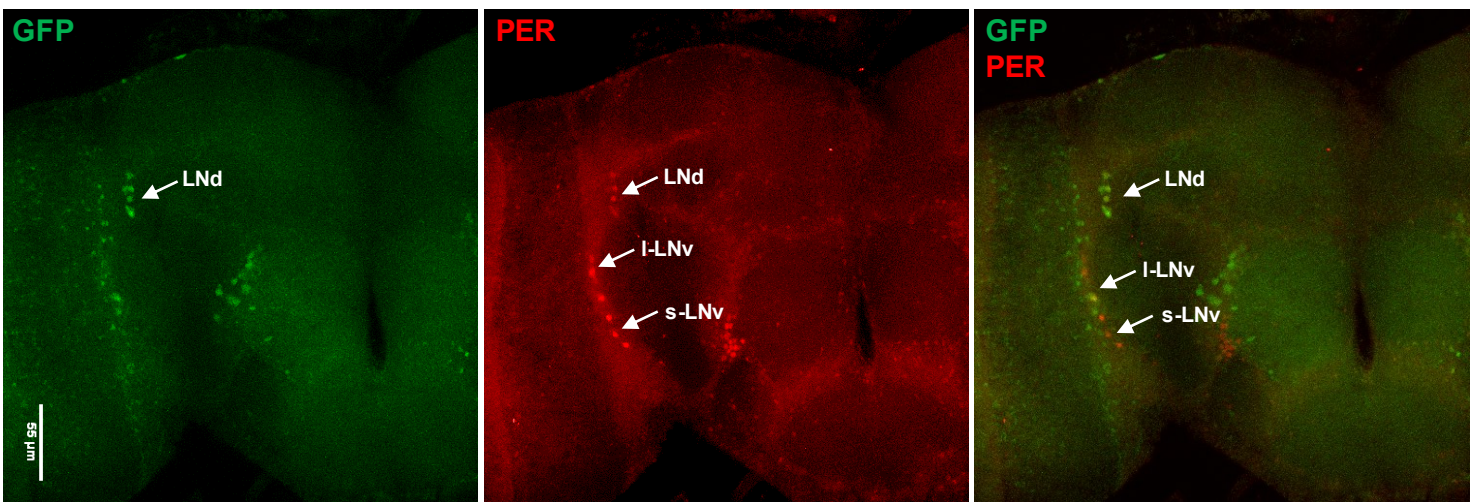


Supplementary fig. S1: Knockdown of *Innexin2* using a different construct (BL 80409) lengthens free-running period, related to Figure 2 (A) Mean free-running period (left) of flies with *Innexin2* downregulated in all clock neurons (*tim; dcr > Inx2* RNAi) ($n=15$) is significantly longer than both its Gal4 ($n=18$) and UAS control ($n=8$) genotypes, (one-way ANOVA, post-hoc Tukey's test, $p < 0.01$) while the power of rhythm (right) is significantly lower from only the Gal4 control, (One-way ANOVA, post-hoc Tukey's test, $p < 0.001$). **(B)** Mean free-running period (left) of flies with *Innexin2* downregulated in all clock neurons (*Clk856 > dcr; Inx2* RNAi) ($n=11$) is significantly longer than both its Gal4 ($n=15$) and UAS control ($n=9$) genotypes, (one-way ANOVA, post-hoc Tukey's test, $p < 0.01$). Power of rhythm of experimental flies is only significantly different from the UAS control flies (One-way ANOVA, post-hoc Tukey's test, $p < 0.001$).

Error bars are SEM, period values are determined using Chi-square periodogram for a period of 8 days. All statistical comparisons were performed using one-way ANOVA with genotype as a fixed factor, followed by post-hoc analysis using Tukey's Honest Significant Difference (HSD) test.

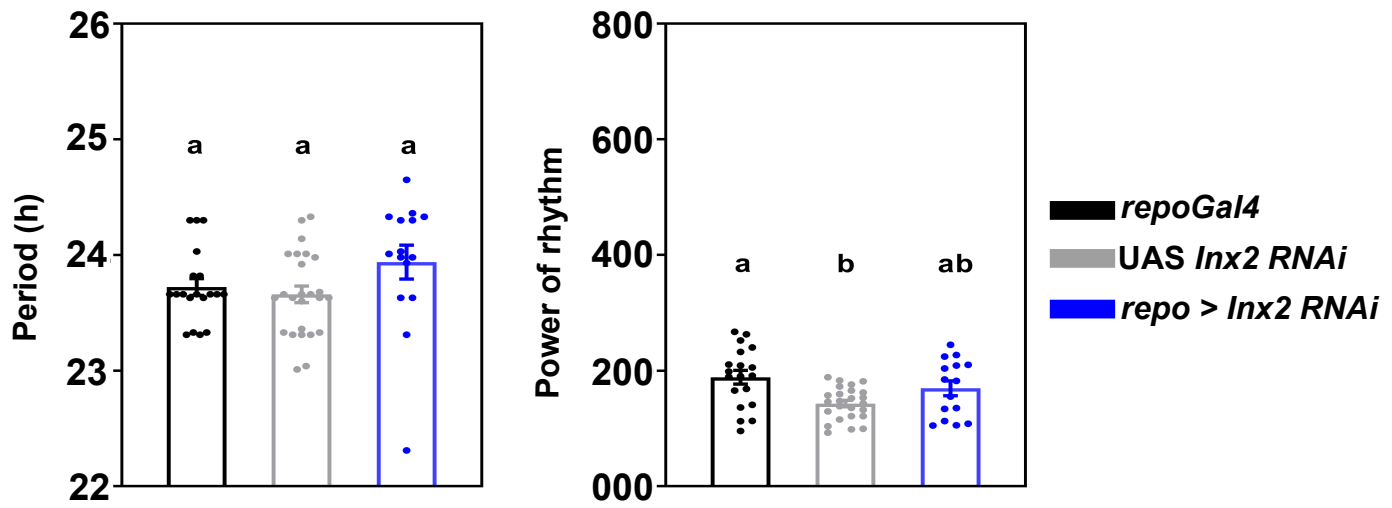


Supplementary fig. S2: Verification of the efficiency of *tubGal80^{ts}* construct, related to Figure 3 (A) The efficiency of *tim; tubGal80^{ts}* construct was verified by crossing with *eGFP*. The flies were reared at a permissive temperature of 19°C. Larvae (L3 stage) from the progeny were dissected and stained with anti-GFP and anti-PER antibodies. s-LNv do not show presence of GFP in permissive temperatures (left), whereas strong PER staining was observed in these cells (middle panel). (B) Adult male flies were transferred to 29°C, 3 days after eclosion, dissected on day 7 and stained with antibodies against GFP and PER. s-LNv, I-LNv and LNds show GFP expression under a restrictive temperature of 29°C. *n*=5 brain samples at each temperature. Scale bars represent 55µm.

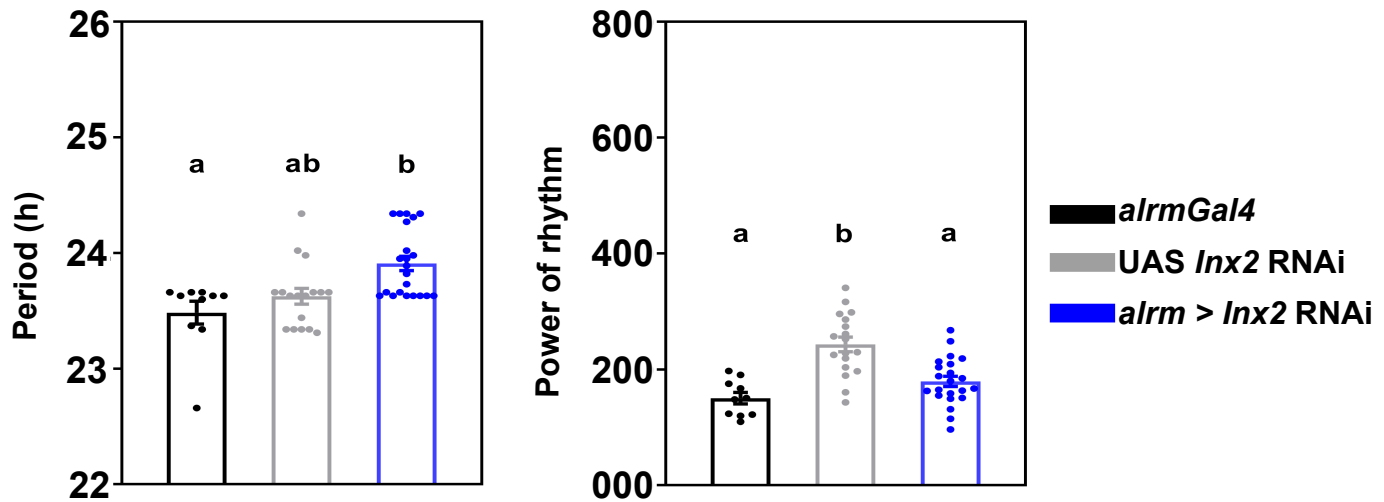
A***LNdGal4 > eGFP*, co-localized with PER****B** ***tim;pdfGal80 > eGFP*, co-localized with PER antibody**

Supplementary fig.S3: Expression pattern of *LNdGal4* and verification of the efficiency of *pdfGal80* construct, related to Figure 4 (A) *LNdGal4 > e-GFP* co-stained with anti-PER antibody shows strong GFP expression in all 6 LNds and faint GFP expression in some I-LNvs as previously reported. No GFP expression was detected in s-LNvs, $n=5$ brain samples. Scale bar represents 110 μ m. (B) The efficiency of *tim; pdfGal80* construct in suppressing *Gal4* driven UAS expression was verified by crossing *timGal4; pdfGal80* with GFP, dissecting the brains at ZT22 and staining with GFP and PER. Both s-LNv and I-LNv did not show any GFP staining (left), whereas PER staining was observed in all lateral clock neurons (middle). $n=6$ brain samples. Scale bars represent 55 μ m.

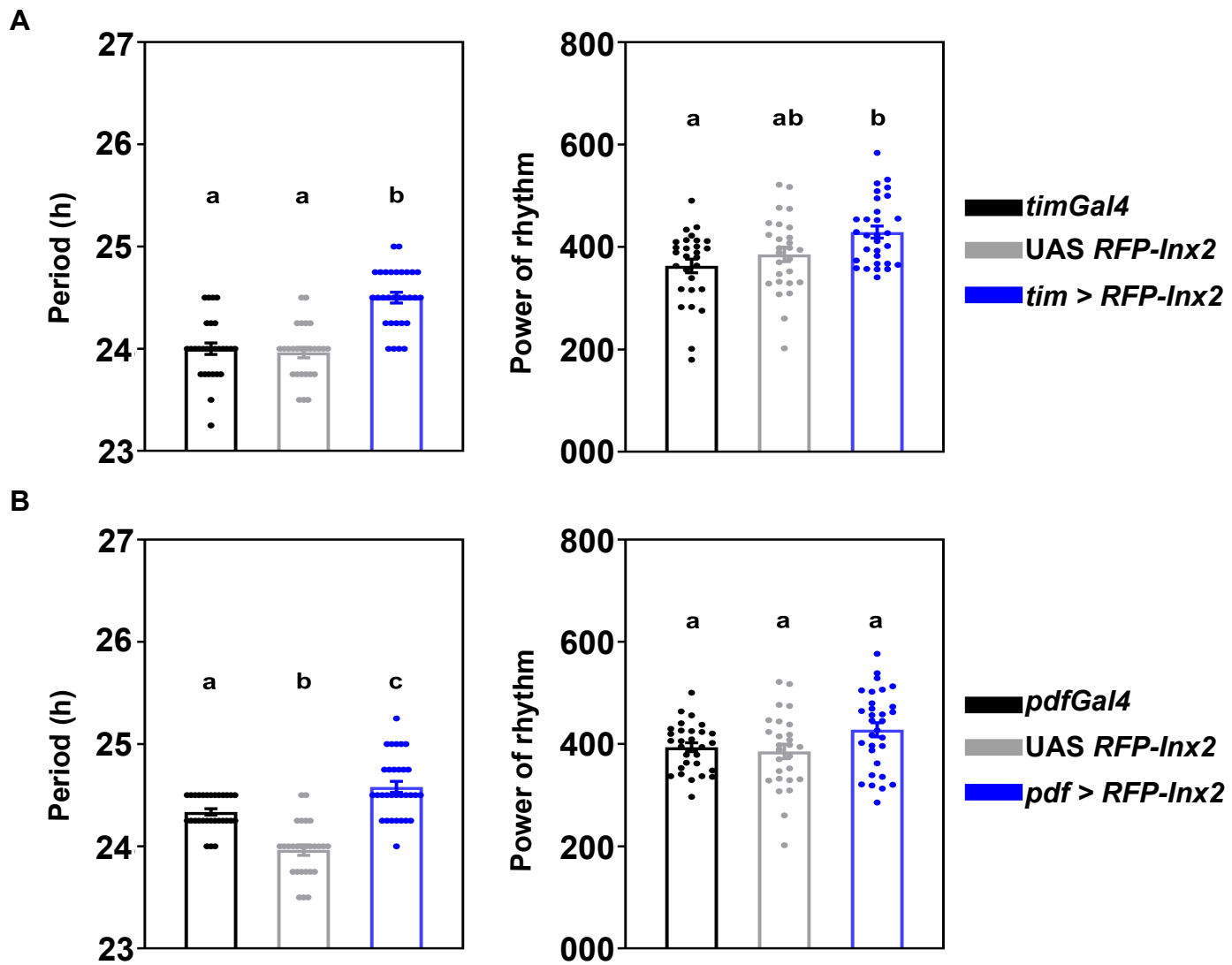
A



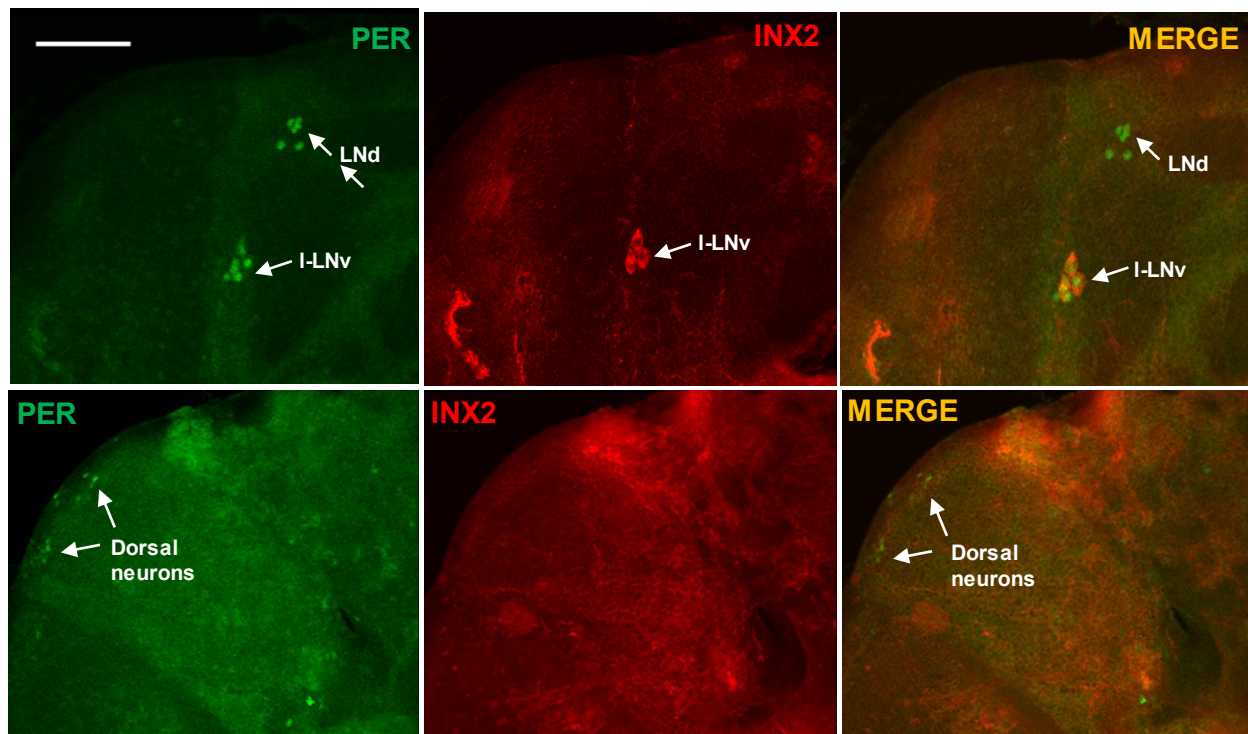
B



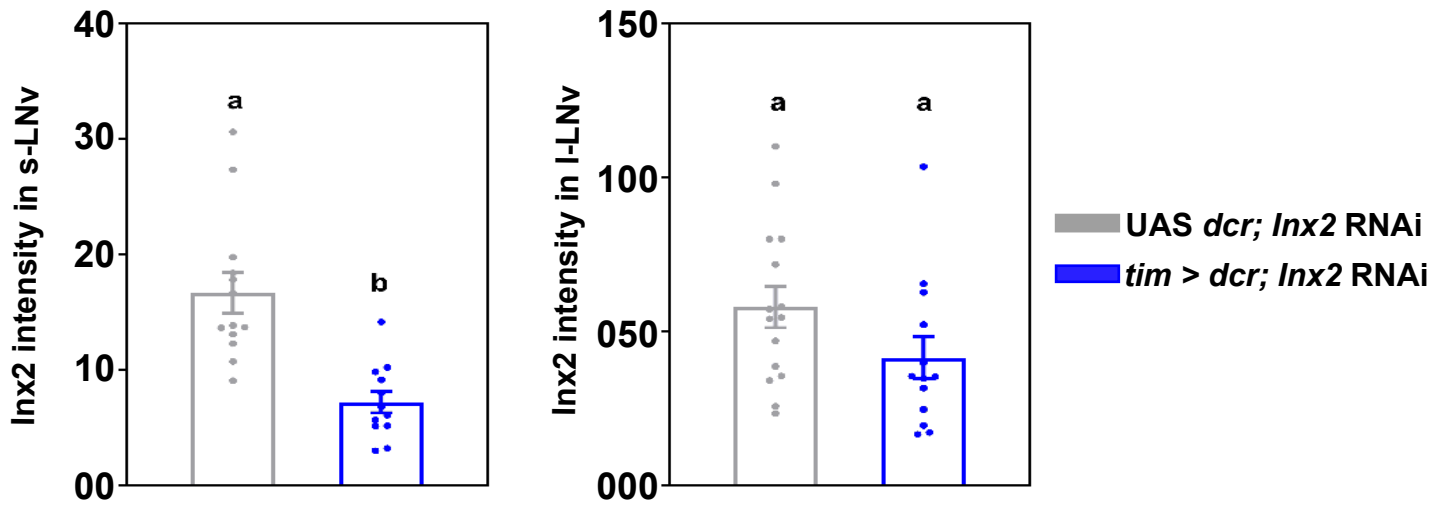
Supplementary fig. S4: Knockdown of *Innexin2* in glial cells does not affect the free-running period, related to Figure 4 (A) Free-running period of experimental flies (*repo > Inx2 RNAi*) ($n=15$) is not significantly different from both its Gal4 ($n=21$) and UAS ($n=25$) parental control flies. Power of rhythm (right) of experimental flies is also not different from its parental control genotypes. (B) Free-running period of experimental flies (*alrm > Inx2 RNAi*) ($n=26$) is only significantly different from its Gal4 control ($n=15$) and not from its UAS parental control ($n=18$) flies (one-way ANOVA followed by post-hoc Tukey's test, $p < 0.01$). Power of rhythm of experimental flies is only different from its UAS parental control (one-way ANOVA followed by post-hoc Tukey's test, $p < 0.001$). Error bars are SEM, period and power values are determined using Chi-square periodogram for a period of 8 days. All statistical comparisons were performed using one-way ANOVA with genotype as a fixed factor, followed by post-hoc analysis using Tukey's Honest Significant Difference (HSD) test.



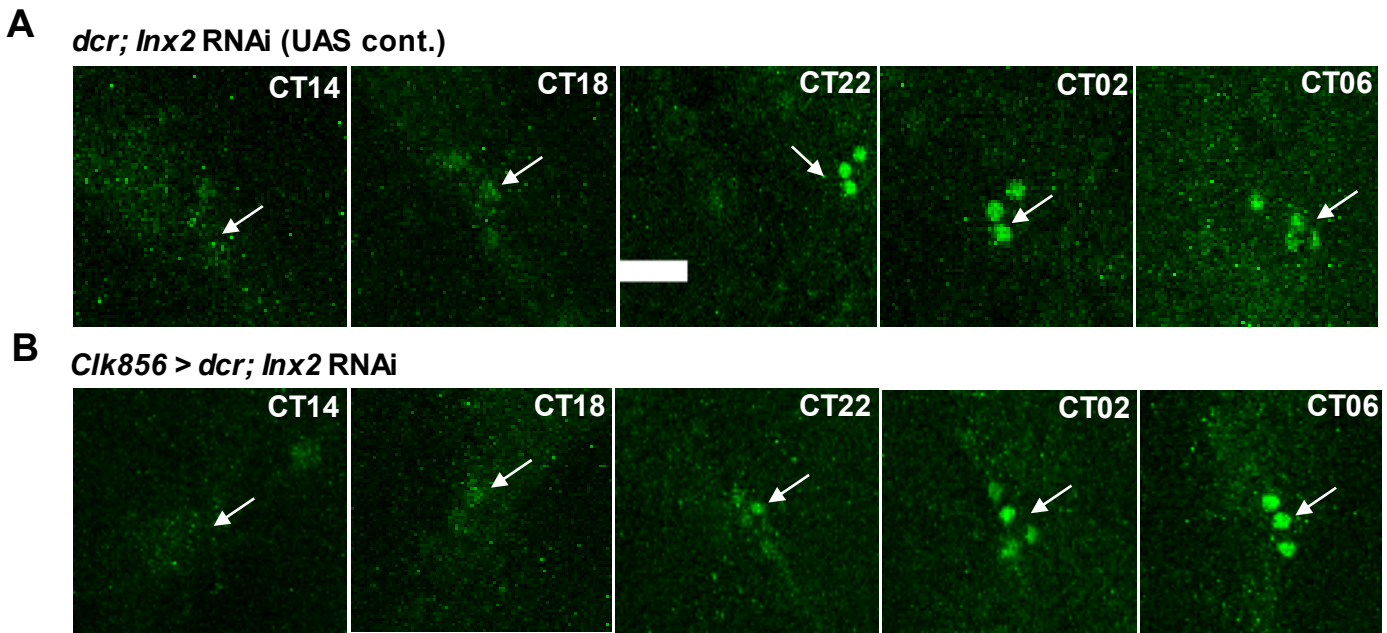
Supplementary fig. S5: Altering the gap junction forming domain of *Innexin2* lengthens free-running period, related to Figure 4 (A) Free-running period of experimental flies (*tim > RFP-Inx2*) ($n=30$) is significantly longer than both its Gal4 ($n=28$) and UAS ($n=27$) parental control flies, (one-way ANOVA, post-hoc Tukey's test, $p < 0.001$). Power of rhythm (right) of experimental flies is only different from its Gal4 control genotype (one-way ANOVA, post-hoc Tukey's test, $p < 0.01$). (B) Free-running period of experimental flies (*pdf > RFP-Inx2*) ($n=31$) is significantly longer than both its Gal4 ($n=29$) and UAS ($n=27$) parental control flies, (one-way ANOVA, post-hoc Tukey's test, $p < 0.001$). Power of rhythm of experimental flies is not different from both its control genotypes. Error bars are SEM, period and power values are determined using Chi-square periodogram for a period of 8 days, All statistical comparisons were performed using one-way ANOVA with genotype as a fixed factor, followed by post-hoc analysis using Tukey's Honest Significant Difference (HSD) test.



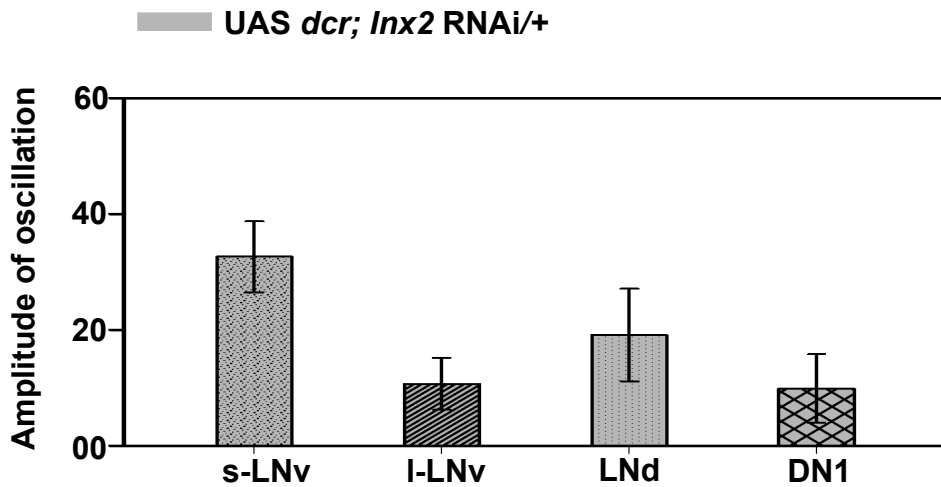
Supplementary fig. S6: Innexin2 is only expressed in the small and large ventral lateral neurons in the circadian pacemaker circuit, related to Figure 5 Representative images from *w¹¹¹⁸* *Drosophila* adult brains showing the distribution of *Inx2* protein among the clock cells. *w¹¹¹⁸* flies were dissected at ZT4 and stained with anti-INX2 antibody and co-stained with anti-PER for identification and co-localization with clock neurons. INX2 was not found to be co-localized with the LNds (top panel) or the DNs (bottom panel). Brightness and contrast of representative images were adjusted in Fiji to facilitate better visualization. Arrows are used to indicate I-LNvs, LNds and DNs. Scale-bar represents 55 μm , $n = 8$ brain samples.



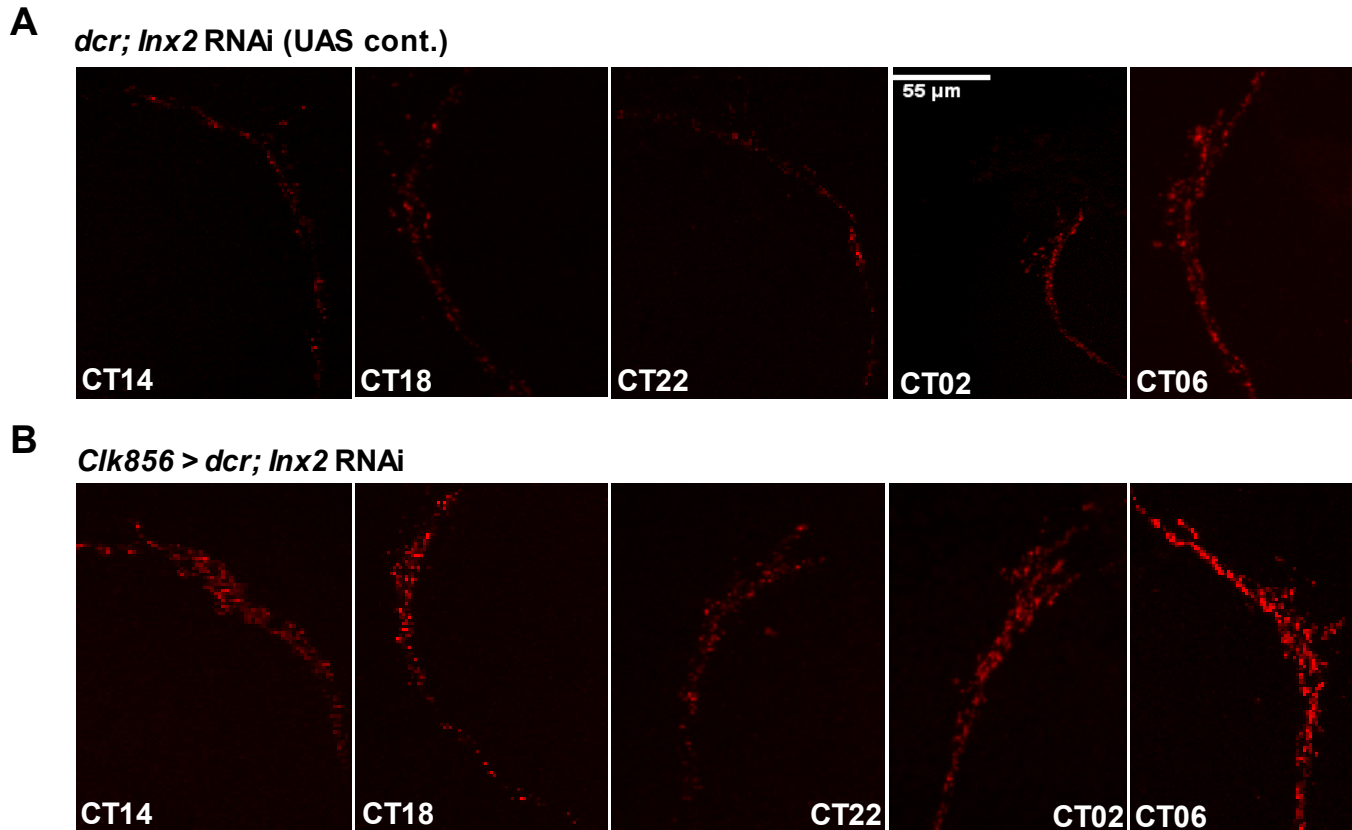
Supplementary fig. S7: Verification of *Innexin2* RNAi, related to Figures 2, 4 and 5 *Innexin2* RNAi construct was verified by dissecting adult brains of both control (*dcr*; *Inx2* RNAi) and experimental flies (*tim* > *dcr*; *Inx2* RNAi) at ZT12 and staining them with anti-INX2 antibody. *Inx2* intensity was quantified in both s-LNVs and I-LNVs and compared between control and experimental flies. *Inx2* levels were lower in s-LNVs (left) in case of experimental flies ($n=12$ brains, Mann Whitney U test, $p < 0.001$). In I-LNVs (right) there was only a decreasing trend observed in *Inx2* levels in experimental flies as compared to control flies ($n=13$ brains, Mann Whitney U test, $p > 0.05$). Error bars are SEM. Each dot represents the mean *Inx2* intensity value for each cell type averaged over both the hemispheres of one brain. The experimental and control genotypes were compared using the Mann-Whitney U test for each cell type.



Supplementary fig. S8: Knockdown of *Innexin2* delays the phase of oscillation of PER protein in s-LNv, related to Figure 6: Representative images of PER intensity in s-LNv at five different time points of a 24-h cycle on the third day of DD 25°C in both control (UAS *dcr Inx2 RNAi*) (**A**) and experimental (*Clk856 > dcr; Inx2 RNAi*) (**B**) flies. Phase of PER oscillations is delayed in brain samples of experimental flies as compared to the control flies. Scale bar represents 55µm.



Supplementary fig. S9: Amplitude of PER oscillations are different in circadian neuronal subsets on third day of DD, related to Figure 6 Amplitude values of PER oscillation in circadian neuronal subsets, obtained from COSINOR curve fits are plotted for control (UAS *dcr*; *Inx2* RNAi) flies. Error bars are 95% CI values calculated from the standard error obtained from COSINOR analysis. Non-overlapping error bars in case of I-LNv, and DN1 compared to s-LNv indicate that these amplitude values are different from s-LNv. COSINOR analysis was implemented using the CATCosinor function from the CATkit package written for R (Lee Gierke and Cornelissen, 2016).



Supplementary fig. S10: Knockdown of *Innexin2* increases the amplitude of PDF cycling in dorsal projections, related to Figure 7 Representative images of PDF intensity in s-LNv dorsal projections at five different time points of a 24-h cycle on third day of DD 25°C in both control (*UAS dcr;Inx2 RNAi*) (**A**) and experimental (*Clk856 > dcr;Inx2 RNAi*) (**B**) flies. Amplitude of PDF oscillation is increased in experimental genotype as compared to the controls. Scale bar represents 55μm.